JOURNAL OF MATERIALS SCIENCE 27 (1992) 335–342

Effect of fibre/matrix interface structure on strength and plasticity of boron aluminium reinforced with discontinuous fibres

L. M. USTINOV, L. A. VERKHOVSKY
A.A. Baikov Institute of Metallurgy, USSR Academy of Sciences, Moscow, USSR

The variation of strength characteristics of boron aluminium were studied in relation to the structure of the fibre–matrix interface. It was found that effects of optimal discrete reinforcement of boron aluminium may be realized to a certain extent if such structural characteristics of the interface as density of interphase bonds, θ, are purposefully changed. In the case where $\theta = 0.340$, the effect of discrete reinforcement is the largest for both failure work and elongation, if the composite strength remains relatively high. Failure work of discrete reinforced boron aluminium is five times higher than that of the continuously reinforced one, but relative elongation reaches ~10%.

1. Introduction

It has been shown [1, 2] that reinforcement of metals with discontinuous brittle fibres is likely to result in greater strengthening, compared to continuous reinforcement. In addition, plasticity and, hence, viscosity of fracture can increase abruptly. According to theory, these effects are realized provided the length of discontinuous fibres is comparable with the critical fibre length and amounts to 2–4 l_{cr} in the case of boron aluminium. The effect of strengthening due to discontinous reinforcement is inversely proportional to the coefficient β although, at the same time, the fibre length at which maximum strength is achieved grows. This is clearly seen in hypothetical boron aluminium whose fibre strength is 3000 MPa (with 20 mm gauge) and diameter is 0.1 mm, the volume fraction being 0.5 and matrix strength 500 MPa [2]. According to these data, for common values of β, the fibre length at which the above effects of discontinuous reinforcement can be expected should not exceed 4–5 mm.

This work describes an effort to verify the experimental conclusions of the theory, particularly where they concern problems of raising the plasticity and work of fracture of boron aluminium.

2. Experimental procedure

The dynamic compaction method of pre-heated evacuated containers with piles of blanks was used to produce unidirectionally reinforced boron aluminium. Plasma-deposited aluminum ADI served as matrix. Flat-stressing test-pieces shaped as double-sided blades were cut out of boron aluminium plates along the reinforcement direction using the electric-arc method. The width, length and thickness of the effective section of the specimens were 3.5, 12 and 2 mm, respectively. The diameter of the boron fibres was 0.13 mm, volume fraction, V_f, 0.33.

To alter the fibre/matrix interface structure in the direction desired, the specimens were annealed in air in a resistance furnace at 400, 500, 520, 550 and 580 °C for 1 h. Boron aluminium, as well as boron etched out of it with 10% KOH solution, were tested in an Instron machine at 1 mm min^{-1} deformation rate. The fibre testing gauge was 25 mm. The boron aluminium discontinuity extent was found experimentally. In fact, the matrix was etched off the boron aluminium in 10% KOH solution, followed by evaluation of the average length of the boron fibres that had been broken at the boron aluminium dynamic compaction stage.

3. Characteristics of discontinuously reinforced boron aluminium stress–strain curve

Fig. 1 and Table 1 contain results of boron aluminium stress–strain tests. They show that boron aluminium strength and plasticity generally do not undergo changes when the annealing temperature is below 500 °C. However, ε_c declines at 500 °C which can be accounted for by random deviation of the plot of ε_c against annealing temperature (Fig. 1). It is of interest that the fracture elongation of the discontinuously reinforced boron aluminium is 10%–12% while that of the continuously reinforced, similarly structured one does not exceed 2–3% (Fig. 2). As the annealing temperature increases further, the boron aluminium strength and plasticity increase noticeably, reaching maximum values at 520 °C; maximum elongation (> 10%) takes place at 520–550 °C. Abrupt decline of these mechanical properties, particularly plasticity (~ 4%), takes place at 580 °C.

An unusually large fracture elongation of boron aluminium seems to be responsible for the unusual shape of its stress–strain curve, which is quite different

0022–2461/92 $03.00 + .12

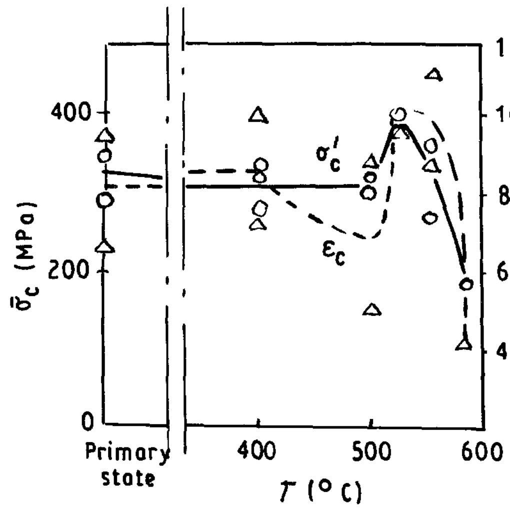

Figure 1 Strength and fracture elongation of discontinuously reinforced boron aluminium versus annealing temperature.

from that of the continuously reinforced boron aluminium. In fact, the stress–strain curve of the discontinuously reinforced boron aluminium possesses six typical stages. They are the initial stage (between points 1 and 2); the elastic deformation stage, where both matrix and fibres undergo elastic deformation; the transient stage (between points 2 and 3) where, at elastic deformation of fibres, the matrix is gradually involved in plastic deformation as the load increases; plasto-elastic deformation stage (between points 3 and 4) where the matrix undergoes plastic deformation and fibres undergo elastic deformation accompanied by clearly audible ruptures that do not yet have any crucial effect on material fracture; the prefracture stage (between points 4 and 5) where, judging by the toothed character of this section of the curve and also by audible signals, fibre ruptures become much greater and is concentrated in the specimen fracture site; the overall boron aluminium fracture stage (between points 5 and 6) characterized by abrupt dip of load which seems to be related to fracture of the matrix in the weakened cross-section of the specimen; the final stage (between points 6 and 7) where fibres are pulled out of the matrix. The latter is characterized by very small stress which is inversely proportional to deformation (see Fig. 3).

From the initial stage and up to the overall fracture stage, stresses grow proportionally to deformation, its intensity, evaluated by the stress–strain curve slope, decreasing in passing from region to region. The stress–strain curves were constructed without using an extensometer, so it was impossible to obtain a reasonably accurate deformation range of the first regions in which the elastic deformation is relatively high, particularly at the first stage of elongation. In stress–strain sections 3–6, i.e. where matrix plastic deformation prevails, the evaluated deformation and, hence, overall fracture elongation, $\varepsilon_c = \varepsilon^{(s)}$, describes the plasticity of the discontinuously reinforced boron aluminium adequately.

The transient stage (section 2) is characterized by gradual decrease of tg α when deformation grows. The plasto-elastic deformation stage (section 3) is the

TABLE I Characteristics of the boron aluminium stress–strain curve

Annealing temperature (°C)	$\sigma_c = \sigma^{(5)}$ (MPa)	$\sigma_c^{(2)}$ (MPa)	$\sigma_c^{(3)}$ (MPa)	$\sigma_c^{(4)}$ (MPa)	$\sigma_c^{(6)-(7)}$ (MPa)	$\varepsilon_c = \varepsilon^{(5)}$	$\Delta\varepsilon^{(3)-(2)}$	$\Delta\varepsilon^{(4)-(3)}$	$\Delta\varepsilon^{(5)-(4)}$	$\Delta\varepsilon^{(7)-(6)}$	tgα_1 (MPa)	tgα_2 (MPa)
Initial	353	139	228	338	10	0.098	0.023	0.054	0.012	0.004	2040	1250
state	294	103	190	262	24	0.066	0.014	0.028	0.017	0.003	2550	1840
400	329	100	179	314	94–93	0.102	0.016	0.063	0.013	0.002	2140	1150
	260	108	180	245	62–50	0.068	0.010	0.038	0.009	0.010	1680	1670
	318	143	238	310	43–40	0.072	0.021	0.039	0.007	0.010	1850	1140
500	300	100	142	288	70–63	0.084	0.007	0.061	0.008	0.009	2380	1500
	312	132	195	300	156–148	0.052	0.012	0.026	0.007	0.003	4040	1710
520	396	124	227	372	68–65	0.100	0.025	0.056	0.010	0.004	2580	2400
550	372	104	174	372	148–130	0.116	0.015	0.094	0	0.003	2110	0
	298	89	145	298	126–105	0.090	0.011	0.073	0.001	0.002	2110	0
580	194	80	153	193	84–57	0.044	0.015	0.021	0.002	0.004	1900	500

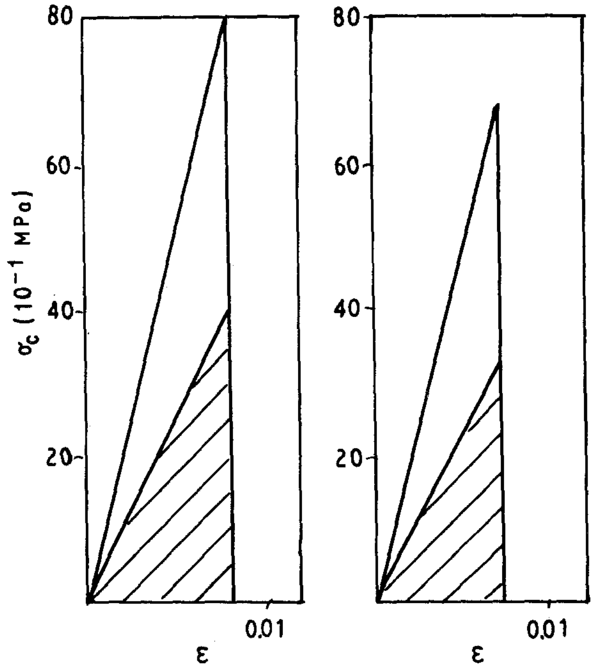

Figure 2 Stress–strain curves of boron aluminium with continuous fibres compacted at 520 and 580 °C. Hatched section corresponds to work of fracture of boron aluminium with $V_f = 0.33$ (calculated).

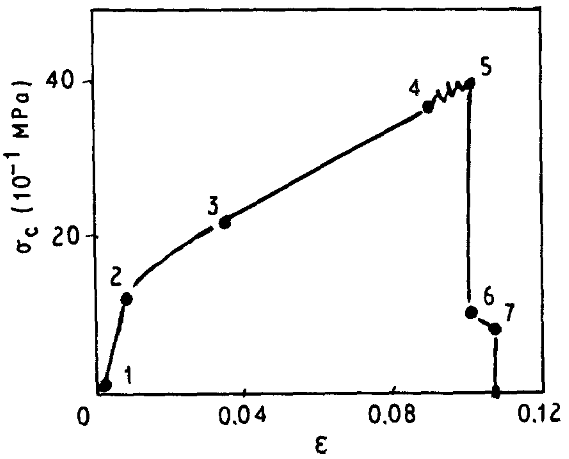

Figure 3 Stress–strain curve of discontinuously reinforced boron aluminium, θ = 0.113.

longest and has a constant slope, i.e. constant deformation hardening coefficient.

The pre-fracture stage, which is rather short, is characterized by a smaller deformation hardening coefficient than the previous one. In boron aluminium annealed at 550 and 580 °C, the pre-fracture stage degenerates. In the final, sixth, stress–strain curve section, the fibres are pulled out of the matrix. The length of this section can be assumed to grow proportionally to the average length of the fibres pulled out of the matrix when rather great friction forces exist between the fibres and the matrix. As the fibres are pulled out of the matrix, the overall specimen load goes down, thus exerting an influence on the generally declining curve trend at this section.

4. Structure and strength of the fibre/matrix interface

The structural state of the fibre/matrix interfaces was evaluated using the planimetric method described in [3]. With this end in view, shear tests of specially prepared boron aluminium specimens were carried out. The area of aluminium pieces stuck to the boron fibres was determined by the surface condition of these fibres that had emerged on the boron aluminium surface due to shear. The ratio of this area and the reinforcing fibre surface, yields the interface bond density, θ. For boron aluminium annealed at 580 °C, θ was determined by the surface of fibres pulled out of the fracture-tested specimens.

As the annealing temperature increases, θ grows, at first (up to 520 °C) slowly and then rapidly reaching the maximum value of 0.57 at 580 °C (Table II and Fig. 4). To find the structural elements influencing the growth of θ, the density, θ_2, of islands of the new phase, boride in this case, was evaluated. On increasing the annealing temperature to 520 °C, θ_2 grows as slowly as θ, and at higher temperatures, as fast as θ. Practically over the entire annealing range, $\theta_2 \simeq \theta$ and, hence, the density of bonding sites, θ_1, found as a difference between θ and θ_2, is zero. It can be concluded from this that annealing of dynamically compacted boron aluminium specimens causes the density of interface bonds to grow, which is due almost entirely to formation and growth of islands of the new phase, i.e. sintering.

The results obtained make it possible to reveal, to a certain extent, the kinetic side of the process in which the fibre and matrix are bound together. We will confine ourselves to evaluation of $\Delta\theta/\Delta T$ ratios that represent the increasing density of both the interface bonds and islands of the new phase. They also characterize the fibre/matrix sintering rate and are found from equations

$$\frac{\Delta\theta}{\Delta T} = \frac{\theta^{(2)} - \theta^{(1)}}{T_2 - T_1} \qquad (1)$$

$$\frac{\Delta\theta_2}{T} = \frac{\theta_2^{(2)} - \theta_2^{(1)}}{T_2 - T_1} \qquad (2)$$

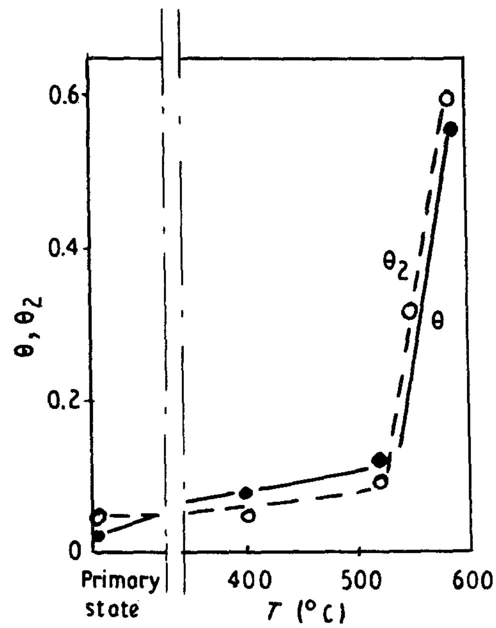

Figure 4 Annealing temperature of discontinuously reinforced boron aluminium versus interface bond density, θ, and density of the new phase, θ_2.

TABLE II Structural and mechanical characteristics of discontinuously reinforced boron aluminium

Annealing temp. (°C)	τ_c (MPa)	θ	θ_2	$\bar{\sigma}_f$ (MPa)	β	τ_m (MPa)	τ (MPa)	l_{cr} (mm)	$\bar{l}_f^*$ (mm)	$\bar{l}_f/\bar{l}_f^*$
Initial state	8.2	0.033	0.040	2910	6.04	36.4	1.2	205	12.9	2.8
400	11.2	0.070	0.063	2440	6.20	45.7	3.2	37.5	10	4
500	–	–	0.083	2160	7.17	–	–	–	11	–
520	11.5	0.113	0.093	2060	6.55	40.0	4.5	26.7	7.6	5
550	12.5	–	0.340	1180	2.26	26.2	8.9	5.56	16.7	2.1
580	–	0.570	0.607	797	2.13	2.3[a]	13.2	1.4	7.7	4.6

[a] Obtained indirectly.

where $\theta^{(2)}$ and $\theta^{(1)}$ are densities of interatomic bonds at annealing temperatures T_2 and T_1, respectively, and $\theta_2^{(2)}$ and $\theta_2^{(1)}$ are densities of islands of the new phase at these temperatures. Calculations showed $\Delta\theta/\Delta T$ and $\Delta\theta_2/\Delta T$ to be 0.35×10^{-4} and 0.17×10^{-4} I K^{-1} within the annealing temperature range 400–500 °C, which is two to three orders of magnitude less than similar characteristics calculated for the 550–580 °C range and equal to 123×10^{-4} and 88×10^{-4} I K^{-1}, respectively.

Similar procedures can be used to evaluate the kinetics of interface structure formation depending on other process parameters, i.e. pressure and time of compaction. Here, we can find an unambiguous relationship between compaction process parameters, interface structure and composite material strength.

Strength and β coefficient of boron fibres extracted from boron aluminium are practically the same in both the unannealed and annealed states up to 520 °C, inclusive. At higher boron aluminium annealing temperatures, $\bar{\sigma}_f$ and β go down markedly, which is directly related to an abrupt increase in the $\Delta\theta_2/\Delta T$ ratio that describes the stage at which the islands of the new phase are growing, in contrast to that at which they originate, the latter being characterized by low values of this term.

Judging by the interface bond density, θ, and boron aluminium interlayer, the interface strength, τ, was found assuming that, as a first approximation, the strength of islands of the new phase is equal to that of the matrix. The known Equation 3 coupled with that of τ versus θ_2 was used for calculation taking into account the given assumption

$$\tau_c = \tau_m \bar{S}_m + \tau \bar{S}_i \quad (3)$$

$$\tau = \tau_m \theta_2 \quad (4)$$

where τ and τ_m are interface and matrix shear strength, respectively; $\bar{S}_m$ is the shear fracture-affected surface area occupied by the matrix in gaps between adjacent fibres; $\bar{S}_i$ is the fracture surface area of fibres ($\bar{S}_i = I - \bar{S}_m$).

Here, besides τ, we will also calculate τ_m. The results are shown in Table II. The distance between the reinforcing layers and fibre diameter was used to calculate $\bar{S}_m$ and $\bar{S}_i$ which were 0.2 and 0.8.

The value of τ grows continuously in proportion to the annealing temperature. However, even its maximum value is several times less than the matrix strength.

5. Effects of discontinuous reinforcement

The average length of fibres etched out of original, 50 mm boron aluminium specimens was $\bar{l}_f = 36$ mm and the critical fibre length, l_{cr}, calculated from Equations 1 and 2 is

$$l_{cr} = \left(\frac{\sigma_f^-(l_1) l_1^{1/\beta} d_f}{2\tau}\right)^{\beta/(1+\beta)} \quad (5)$$

where σ_f^- (l_1) is the average strength of l_1-based fibres (25 mm); d_f is the fibre diameter (see Table II). The boron aluminium reinforcement discontinuity extent is found from the $\bar{l}_f/l_{cr}$ ratio. According to theory, the effect of discontinuous reinforcement to enhance the boron aluminium strength must be noticeable with $\bar{l}_f/l_{cr}$ being not more than ~ 6 for $\beta = 2$–6 [1, 2]. Thus, we can conclude that, keeping in mind $\bar{l}_f/l_{cr}$ and the specimen length as a first approximation, the boron aluminium annealed at temperatures below 550 and 580 °C can be taken as the discontinuously reinforced one.

With boron aluminium being strained at the plasto-elastic deformation stage, the fibres are continuously broken into shorter lengths. This process occurs, largely, as a result of friction forces that exist between the fibres and matrix and are not taken into account here. Thus, while approaching the pre-fracture stage, the fibres become shorter and shorter and, therefore, in conformity with the scale effect, stronger and stronger. Each following fibre break requires greater stress. It is this fact that accounts for the slope of the curve whose angle characterizes the work hardening coefficient at the plasto-elastic deformation stage. It goes without saying that, in this case, the nature of the work hardening coefficient is quite different from that of metals and alloys.

It is of interest to stress that the breaking process occurs in boron aluminium with a rather large volume fraction of fibres ($V_f = 0.33$). This unusual fact is accounted for by low interface bond density, owing to which fibre failures seem to be localized as a result of its separation from the matrix in this particular place due to the poor interface. In other words, individual fibre fracture has no effect on fracture of adjacent ones occurring as a result of the concentration of stresses and matrix deformation in the place of fracture. Only when the total quantity of cracks in some local specimen volume reaches a certain "critical" value, does its deformation in this volume start to become localized. This is where the pre-fracture stage begins in which the fibres are being ruptured intensely by the overload mechanism until general specimen fracture is achieved.

As the interface bond density increases, the length of the plasto-elastic deformation stage, $\Delta\varepsilon^{(4)-(3)}$, grows from 4% to 8% at $\theta = 0.340$; afterwards, it drops abruptly to 2% at $\theta = 0.570$, while the length of the pre-fracture stage, $\Delta\varepsilon^{(5)-(4)}$, decreases continuously from $\sim 1.5\%$ at $\theta = 0.033$ to almost zero at $\theta = 0.340$ (Fig. 5).

The work hardening coefficient at the composite plasto-elastic deformation stage, tg α, at first grows almost two-fold proportionally to θ (at $\theta = \theta_2 = 0.083$) and then drops back to the initial level (Fig. 6). This growth seems to be due to the most favourable fibre breaking conditions existing at $\theta = 0.083$. As the work hardening coefficient grows, the composite plasto-elastic deformation stage decreases slightly (Table I). An almost similar dependence of work hardening coefficient on θ also exists at the pre-fracture stage (Fig. 6). This points to the fact that the main reason for work hardening at both stages is the fibre breaking process. It has already been mentioned that the pre-fracture stage is characterized by localized deformation and fracture that occur within the so-called characteristic length l_{ch} which is equal to $0.25\,l_{cr}$, as shown by Shoshorov *et al.* [4, 5]. With l_{cr} decreased, l_{ch} decreases as well, as do $\Delta\ l_{ch}$ and $\Delta\varepsilon^{(5)-(4)}$, equal to the specimen testing gauge (Fig. 7).

The boron aluminium reinforcement discontinuity is inversely proportional to θ, as the $\bar{l}_f/l_{cr}$ ratio increases from 0.170 to 25.7 (Fig. 8). In fact, due to breaking of fibres during boron aluminium straining, the discontinuity of reinforcement increases. Analysis of broken specimens showed that prior to fracture the discontinuity of the specimen fibrous structure grows, because the $\bar{l}_f^*/l_{cr}$ ratio goes down two to five fold as compared with $\bar{l}_f/l_{cr}$. The increase in θ results in the $\bar{l}_f^*/l_{cr}$ ratio increasing to a maximum equal to 6 at $\theta = 0.570$ (Fig. 8).

The stress–strain-tested boron aluminium can be treated as a composite discontinuously reinforced

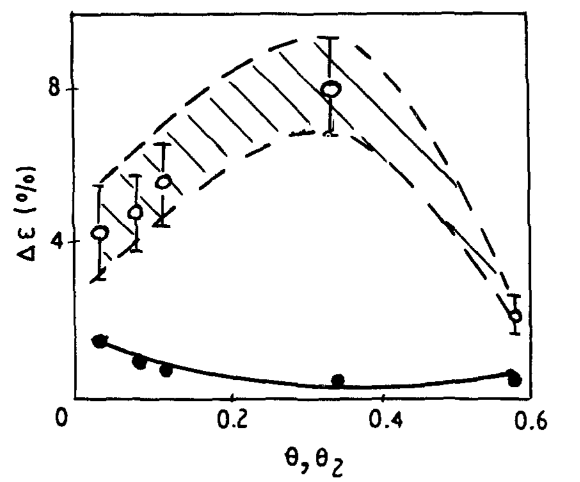

Figure 5 Lengths of the plasto-elastic deformation, (○) $\Delta\varepsilon^{(4)-(3)}$, and pre-fracture, (●) $\Delta\varepsilon^{(5)-(4)}$, stages versus interface bond density, θ.

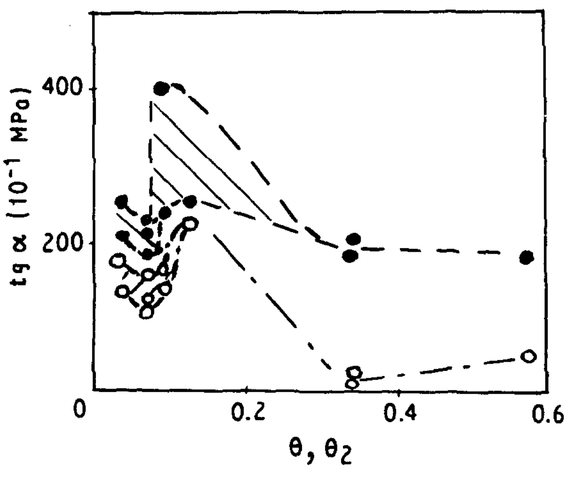

Figure 6 Work hardening coefficients at plasto-elastic, (●) tg α_1, and pre-fracture, (○) tg α_2, stages versus interface bond density.

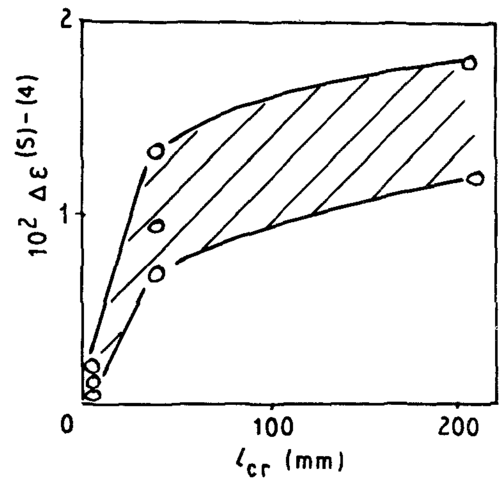

Figure 7 Length of the pre-fracture, $\Delta\varepsilon^{(5)-(4)}$, stage versus critical fibre length, l_{cr}.

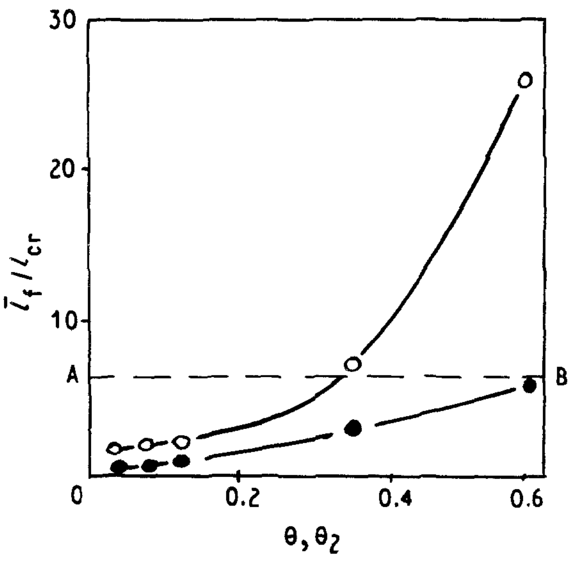

Figure 8 Extent of boron aluminium reinforcement discontinuity versus interface bond density in the initial state, (○) $\bar{l}_f/l_{cr}$, and after break-test, (●) $\bar{l}_f^*/l_{cr}$.

with fibres whose average length is close to optimum [2]. However, there must exist a reservation that the plasticity of the matrix of this composite has been partially exhausted. In addition, the material is saturated with pores and cracks formed as a result of fibre breakage. Therefore, to take full advantage of discontinuous reinforcement to achieve both maximum strength and plasticity seems to be impossible.

With $\theta = 0.340$, the boron aluminium has maximum strength because, in this case, boron fibres are not only relatively strong, but also have a low coefficient β (close to 2); according to theory [2], this yields the greatest strengthening effect of discontinuous reinforcement.

The $\bar{l}_f/\bar{l}_f^*$ ratio describes not only the intensity of fibre breakage during stressing of a composite material, but also its defectiveness, i.e. the specific number of pores and cracks formed as a result of fibre breakage. On the one hand, the fibre breakage process resulting in a more optimum variant of discontinuous reinforcement improves the material plasticity, while, on the other hand, an unfavourable tendency from this mechanical property (i.e. greater defectiveness) manifests itself more vividly. Thus, it becomes clear why maximum plasticity is achieved at minimum breakage intensity occurring at $\theta = 0.340$ (Fig. 9).

The discontinuous reinforcement effect manifests itself in one way or another in practically all specimens, the maximum plasticity and strength being achieved at $\theta = 0.340$ (Fig. 10).

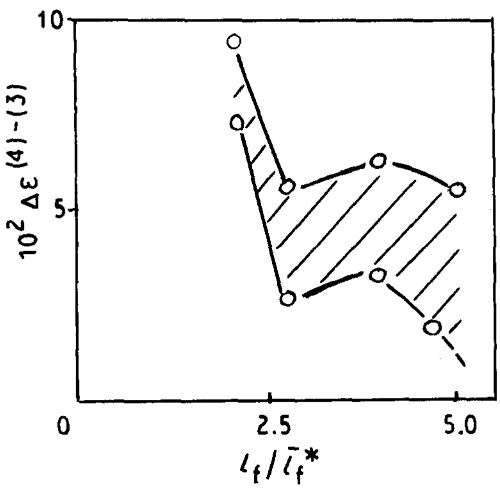

Figure 9 Fibre breakage intensity, $\bar{l}_f/\bar{l}_f^*$, versus length of plasto-elastic deformation stage, $\Delta\varepsilon^{(4)-(3)}$.

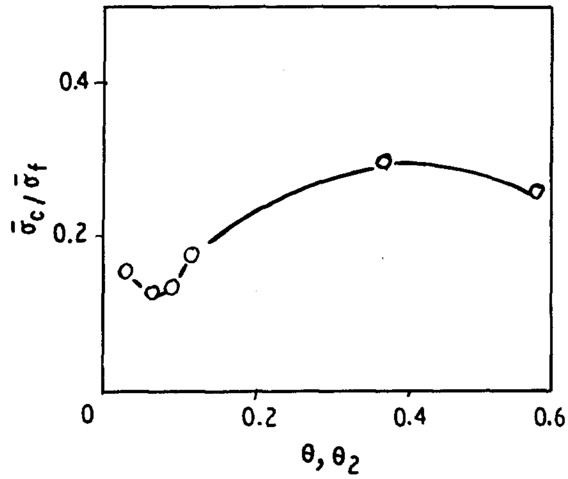

Figure 10 Relative strength of discontinuously reinforced boron aluminium, $\sigma_c/\bar{\sigma}_f$, versus interface bond density, θ.

6. Work of fracture

According to the theory, optimum reinforcement with discontinuous fibres improves the composite strength and plasticity and, therefore, work of fracture. We will illustrate this by a concrete example. Using the stress–strain curve we can determine the work of fracture of discontinuously and continuously reinforced boron aluminium, as well as ADI aluminium matrix, plasma-deposited and compacted to 100%. According to Shorshorov *et al.* [6], the matrix stress–strain curve at the plastic deformation section is practically linear; the yield point and ultimate tensile strength are ~ 30 and ~ 80 MPa, respectively, and fracture elongation is $\sim 25\%$. The area under the stress–strain curve in σ–ε coordinates, which we mark as W (mm^2), will be taken as the conventional characteristic of the work of fracture of the material.

Calculations showed that the work of fracture of the discontinuously reinforced boron aluminium generally grows proportionally to θ and reaches a maximum at $\theta = 0.340$; after that it declines abruptly (Fig. 11 and Table III). The contribution of the last stage of fracture of discontinuously reinforced boron aluminium (when fibres are pulled out of the matrix) to the total work of fracture, is relatively small and does not exceed 3%–4% W (Table III). With θ growing, W_p grows to maximum at $\theta = 0.113$ and then decreases, slowly at first and then very rapidly at $\theta > 0.340$.

Comparing the characters of W and W_p with θ and θ_2, we can claim that the highest values of W and W_p seem to lie somewhere between those of θ and θ_2 equal

TABLE III Work of fracture of discontinuously reinforced boron aluminium

θ; θ_2	$\bar{l}_f/l_{cr}$	$\bar{l}_f^*/l_{cr}$	W (mm^2)	W_p (mm^2)	$W_p/W \times 100\%$	$\bar{l}_f^{**}$ (mm)	$\bar{l}_f^{**}/d_f$	l_{cr}/d_f
0.033	0.170	0.06	4850	12	0.25	13.25	103.8	1577
0.070	1.04	0.26	4575	55	1.20	8.62	66.3	288
0.083	–	–	3475	107	3.08	5.62	43.2	–
0.113	1.35	0.28	5328	115	2.16	5.80	44.6	205
0.340	6.4	3.00	5700	113	2.00	5.22	40.1	43
0.570	25.7	5.5	1300	50	3.84	2.96	22.8	11

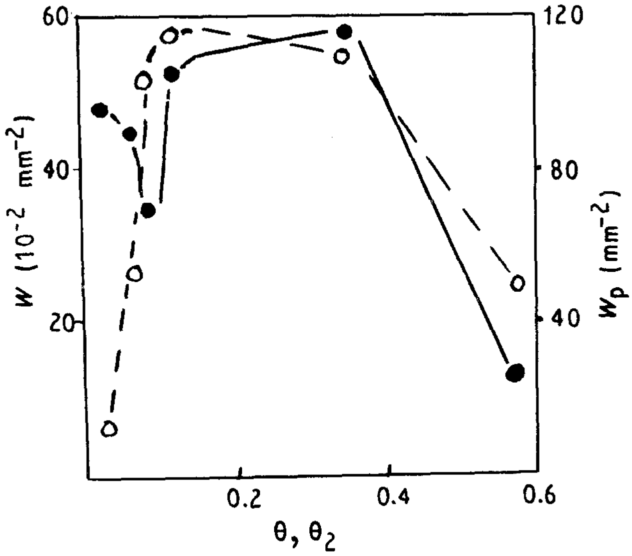

Figure 11 Conventional work of fracture of discontinuously reinforced boron aluminium versus θ. (●) Total work of fracture, W; (○) work of fracture performed at the stage when fibres are pulled out of the matrix, W_p.

to 0.113 and 0.340. The main reason for the abrupt decline of W and W_p at $\theta = \theta_2 = 0.570$ lies in both great reduction in plasticity and loss of fibre strength, resulting in a similarly striking reduction of its critical length. Thus, the material no longer behaves like that optimally reinforced with discontinuous fibres characterized by l_f/l_{cr} of 2–6. This is in agreement with experimental data on l_f/l_{cr} and $\bar{l}_f^*/l_{cr}$ that describe the extent of discontinuous reinforcement of boron aluminium investigated in this study (Table III).

In studying the boron aluminium fracture surface it was noticed that, with increase of θ and θ_2, the average length of l_f^{**} fibres pulled out of the matrix, decreases. To give quantitative evaluation of this dependence, use was made of ×4–×8 magnified photographs of the boron aluminium fracture surface profile. The average length of $\bar{l}_f^{**}$ fibres pulled out of the matrix was found by direct measurement. It must be admitted that the average length of pulled out fibres seems to be related to the critical fibre length through a certain dependence, because with growth of θ and θ_2, both characteristics decrease monotonically (Table III). The l_{cr}/d_f versus $\bar{l}_f^{**}/d_f$ curve plotted on logarithmic coordinates has the form of a straight line corresponding to the equation

$$l_{cr}/d_f \quad = \quad a(\bar{l}_f^{**}/d_f)^n \qquad (6)$$

where $a = 5 \times 10^{-8}$ and $n = 3.11$, both having been found by the method of least squares. This semi-empirical equation is probably true for cases when the boron aluminium fracture is of a relatively viscous, cumulative character, which agrees with moderate θ values. This equation can be used for evaluation of the critical fibre length by the boron aluminium fractography, although with certain limitations, e.g. with $\bar{l}_f^{**}/d_f$ not greater than ~ 104 and not less than ~ 23, i.e. extreme values used as a basis on which the equation was derived.

Let us compare the work of fracture of discontinuously and continuously reinforced boron aluminium whose stress–strain curve is shown in Fig. 2. The volume fraction of fibres is almost twice as great in the latter as in the former. This must be kept in mind in evaluation of W of the discontinuously reinforced material.

Assuming that fibres make the greatest contribution to the boron aluminium strength, and fracture elongation is practically identical in boron aluminium with $V_f = 0.33$ and 0.60, we will construct a hypothetical stress–strain curve of continuously reinforced composite with $V_f = 0.33$ (Fig. 2) whose fibre strength, according to Shorshorov *et al.* [3], is 1950 MPa (compacted at 580 °C). Let us compare it with the discontinuously reinforced boron aluminium whose fibres have similar strength, i.e. with composite annealed at 520 °C, where $\bar{\sigma}_f = 2060$ MPa. The work of fracture of discontinuously reinforced boron aluminium expressed in conventional units W is 5328 mm^2, i.e. approximately five times as large as that of continuously reinforced material with effective fibre volume fraction, i.e. 1015 mm^2.

The work of fracture of the plasma-deposited and hot-compacted aluminium ADI can be evaluated by the conventional characteristic W which is almost half the size of that of the discontinuously reinforced one and is 2875 mm^2.

It must be stressed that the strength of the discontinuously reinforced boron aluminium is very similar to that of the continuously reinforced one, having an equivalent fibre volume fraction $V_f = 0.33$.

The experimental results shown above were obtained on the material in which all the advantages of discontinuous reinforcement were not made use of, because some of the conditions had not been met. Among other things, fibres of the same specimen differed in length, and when the average fibre length was close to the optimum value, the relatively high vulnerability of the material to damage, due to breaking of fibres, prevented full realization of the effect of strengthening by discontinuous fibres.

7. Conclusions

1. A moderate fibre/matrix interface density provides for partial use of the effects of reinforcement by discontinuous fibres.

2. With an interface bond density of 0.340 and a fibre volume fraction of 0.33, maximum strength and fracture elongation (10%–12%) are achieved. The work of fracture of the discontinuously reinforced boron aluminium is five times that of the continuously reinforced material and twice that of the matrix fracture work.

3. The stress–strain curve of the discontinuously reinforced material with a moderate interface bond density ($\theta < 0.540$) comprises five sections characterized by specific deformation and fracture mechanisms.

4. The stress–strain curve section corresponding to the composite plasto-elastic deformation stage provides for maximum contribution to total elongation and has a linear character, i.e. constant work hardening coefficient whose nature depends on the intensity of fibre breakage into shorter, and, hence, stronger sections.

5. With increasing boron aluminium annealing temperature, the interface bond density increases due to increasing density of islands of the new phase.

6. With increase of the annealing temperature above 520 °C, the boron aluminium strength declines, due to great loss of fibre strength which can be accounted for by the presence of islands of the new phase at the fibre/matrix interface.

7. Stressing of the discontinuously reinforced boron aluminium having great volume fraction ($V_f = 0.33$) and moderate interface bond density, gives rise to further breakage of fibres; as a result, structural characteristics of the material are very close to discontinuous reinforcement conditions.

8. The increase in the average length of the fibres pulled out of the matrix is inversely proportional to the interface bond density and proportional to the critical fibre length in logarithmic coordinates.

References

1. L. M. USTINOV, M. KH. SHORSHOROV and YU. G. KUZNETSOV, *Dokl. ANSSSR* **220** (1975) 1074 (in Russian).
2. M. KH. SHORSHOROV, L. M. USTINOV and YU. G. KUZNETSOV, in "Proceedings of the 1975 International Conference on Composite Materials" edited by E. Scala, E. Anderson, I. Toth and B. R. Noton (AIME, Warrendale PA, 1976) pp. 644–50.
3. M. KH. SHORSHOROV, L. M. USTINOV, L. A. VERKHOVSKY and L. E. GUKASYAN, *Fiz. Khim. Obrabotki Materialov* (3) (1982) 80 (in Russian).
4. M. KH. SHORSHOROV, L. E. GUKASYAN and L. M. USTINOV, *Metall Termich. Obrabotka Metallov* (II) (1980) 22 (in Russian).
5. M. KH. SHORSHOROV, L. M. USTINOV, L. E. GUKASYAN, L. V. VINOGRADOV and L. A. VERKHOVSKY, *Rev. Chim. Minerale* **18**(5) (1981) 427.
6. M. KH. SHORSHOROV, V. V. KUDINOV, V. I. KALITA and S. I. BULYCHEV, (I) (1981) 90 (in Russian).

Received 18 December 1989
and accepted 24 April 1991